Interaction of 3.7-Mev Neutrons with Medium Weight Nuclei*

D. W. KENT, S. P. PURI,† S. C. SNOWDON,‡ AND W. P. BUCHER
Bartol Research Foundation of the Franklin Institute, Swarthmore, Pennsylvania
(Received August 29, 1961)

A beam of 3.7-Mev neutrons having an energy spread of 400 kev has been used to measure the differential cross sections of calcium, potassium, germanium, selenium, and strontium. Nonelastic cross sections are obtained by subtracting integrated elastic cross sections from the total cross sections. In addition, measurements of the transmission for ten additional elements have been made at this energy as part of a comparison of total cross sections with optical-model predictions for medium weight nuclei.

I. INTRODUCTION

INTERPRETATION of nuclear properties by means of an optical model entails experimental determination of differential and integrated cross sections as well as azimuthal asymmetries observed in nucleon-nucleus scattering. Thus, inclusion of a spin-orbit coupling term in the nuclear potential has improved predictions of data obtained in several cases of fast-neutron scattering.[1] The data presented here are results of a continuation of our experimental investigation of scattering from medium weight nuclei with the neutron energy fixed at 3.7 Mev. Differential and integrated cross sections for five elements are presented, and measurements of total cross sections for ten additional elements are included. Since the energy of the neutron beam is distributed over a range of 400 kev, the main condition is fulfilled for an optical model representation where many levels in the compound nucleus are involved. The experimental arrangement, which has been discussed in earlier papers,[2] permits good angular resolution and discrimination against γ rays by limiting the size of the detector crystal.

II. EXPERIMENTAL DETAILS

Bombardment by 1.0-Mev deuterons of a gas cell containing 1.8 cm^3 of deuterium at a constant 1.0-atmosphere pressure produced a neutron beam having a mean energy of 3.66 Mev in the forward direction.[2] A 45-μamp deuteron beam intensity was maintained, using simple water-evaporation cooling of the nickel foil mount. Detection was restricted to elastically scattered neutrons by observing the upper portion of the pulse-height distribution from proton recoils in a 0.1-in. diam by 0.1-in. high cylinder of plastic scintillant fixed to the face of a $\frac{3}{4}$-in. diameter phototube. Pulses from the anode, together with a test pulse inserted in the cathode follower, were amplified and fed to a 100-channel analyzer. Since most of the data required comparison between runs having the same neutron beam flux within limits of a few percent, a stable neutron monitor was essential. For this purpose a detection system nearly identical to the one just described was used, except that a single-channel analyzer selected the upper 25% of the pulse-height spectrum, while excluding the test pulse. For angular distribution measurements, the elements to be studied were cast in the form of 3-in., 5-in., and 7-in. mean diameter annular rings, with cross-sectional areas 0.7–1.0 in.^{2} Isolation of the detector from direct neutrons during scatterer-in and scatterer-out runs was obtained by using a 1-in. diam by 8-in. long tungsten attenuator in a geometry designed to minimize interference with the scattered beam by multiple scattering processes. The scattering angle was varied in fourteen steps from 10° to 150° by lateral movement of appropriate rings along the source-detector axis.

III. DATA REDUCTION

Pulse-height distributions of scattered, background, and direct neutrons were modified by empirically determined channel efficiency parameters in order to obtain a corrected ratio of scattered to direct counts for each channel. By restricting attention to the upper 20–30% of the pulse-height spectrum, a mean value of the scattering ratio for elastically scattered neutrons is obtained. The precise number of useful channels available, and hence the statistical accuracy in determining a mean scattering ratio, is determined by judging the position in the pulse-height spectrum at which contributions from gamma rays or nonelastic scattered neutrons appear to become appreciable. This mean scattering ratio is reduced to a differential cross section by appropriate normalization and application of geometrical and multiple scattering corrections. We adopted a simple analytical technique for multiple scattering, based on the assumption that all but one of the multiple scatters are in the forward direction. Angular resolution corrections were calculated using an expansion about the mean trajectory of point-source neutrons scattered from a finite ring into a point detector.

Total cross sections were measured in a conventional transmission geometry, with the same detector and attenuator used for angular distribution measurements.

* Assisted by the U. S. Atomic Energy Commission.
† Research Fellow, 1958–1959 Bartol Research Foundation, now at the University of Alabama, University, Alabama.
‡ Now at Midwestern Universities Research Association, Madison, Wisconsin.
[1] F. E. Bjorklund and S. Fernbach, Phys. Rev. **109**, 1295 (1958).
[2] M. K. Machwe, D. W. Kent, and S. C. Snowdon, Phys. Rev. **114**, 1563 (1959).

TABLE I. Legendre coefficient B_L in $\sigma(x)=(1/4\pi)\ \Sigma\ (2L+1)B_LP_L(x)$. Units of $\sigma(x)$ are barns per steradian.

L	K	Ca	Ge	Se	Sr	Zr
0	2.955±0.215	3.202±0.226	1.780±0.096	1.921±0.201	2.744±0.236	2.142±0.179
1	1.231±0.137	1.319±0.140	1.075±0.059	1.072±0.086	1.096±0.139	0.910±0.082
2	1.046±0.168	1.145±0.180	0.887±0.074	0.807±0.161	1.029±0.193	0.614±0.041
3	0.429±0.090	0.460±0.100	0.595±0.033	0.557±0.055	0.560±0.102	0.331±0.052
4	0.174±0.096	0.195±0.108	0.405±0.018	0.430±0.092	0.654±0.115	0.398±0.088
5	0.062±0.046	0.041±0.056	0.133±0.015	0.158±0.026	0.325±0.059	0.213±0.025
6	0.023±0.037	0.012±0.042	0.035±0.014	0.032±0.023	0.136±0.044	0.053±0.022

In most cases the scatterers consisted of 1.0-in. diameter by 1.0-in. long cylinders. Scattering-in usually required a correction of less than 2% of the total cross section. The final integrated elastic cross section was obtained by an iterative procedure in which integration of the original differential cross section, carried out with an approximate value for the nonelastic cross section, is subtracted from the total cross-section measurement.

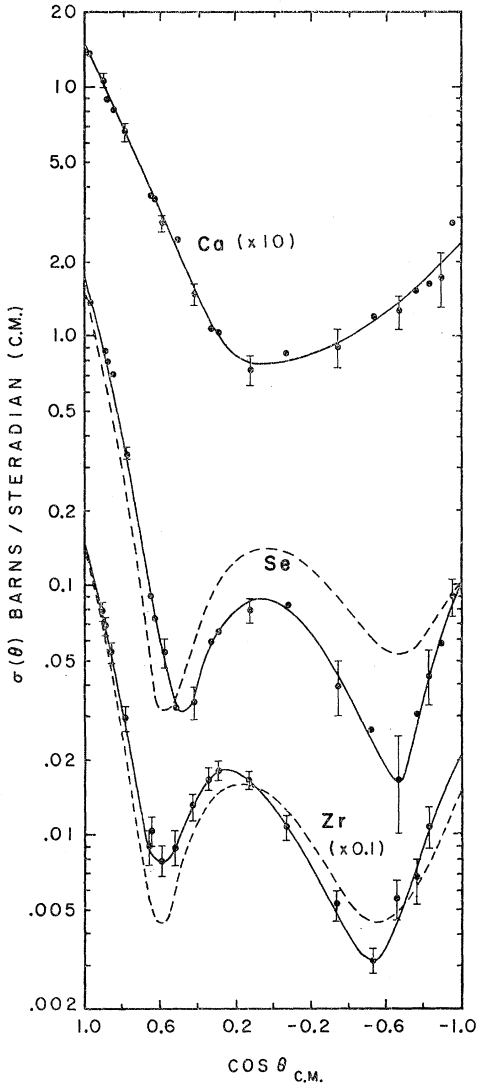

FIG. 1. Differential cross section for elastic scattering of 3.7-Mev neutrons from Ca, Se, and Zr. The solid curves are drawn for use in determining the Legendre coefficients in Table I. The dashed curves are preliminary fits for Se and Zr by Bjorklund $\sigma_{ce}(\theta)=0.03$ barn/steradian. Error bars are shown only on typical points to avoid cluttering of figure.

Apart from purely statistical errors in the scattered flux, several other uncertainties were incorporated into final errors of the angular distribution data. Experimental reproducibility was deduced from three-fold repetition of the measurements, this external measure of the uncertainties exceeding the statistical error by a factor three on the average. The remaining errors were estimated to be the following: (a) Multiple scattering (5%). For zirconium, a correction using the approximation described above compares favorably with that derived from a Monte Carlo procedure, and was therefore applied uniformly to all elements, with an estimated uncertainty given in the bracket. (b) Angular resolution (less than 2%). (c) Systematic asymmetries (4%). No precise correction could be made for this effect. For instance, in the absence of detailed knowledge of the spin-orbit coupling for each neutron-nucleus interaction, polarization corrections are generally undetermined within a limit represented by the above value. The final error in each measurement was a root-mean-square combination of these uncertainties, with the statistical error multiplied by an average reproducibility factor. In the case of total cross-section measurements, the over-all error is dominated by the reproducibility. In some instances, where only relatively thin samples were available, transmissions were as high as 0.85, so that final errors were as large as 7%.

IV. DATA

A. Differential Cross Sections

Angular distributions of the differential cross section for elastic scattering are shown in Figs. 1 and 2 for the five newly measured elements. Representation of the data in terms of Legendre polynomials, using an eleven-point Lagrangian interpolation,[3] is presented in Table I through the first six coefficients in the expression

$$\sigma(x)=(1/4\pi)\ \Sigma\ (2L+1)B_LP_L(x),$$

where $x=\cos\theta$, and θ is the angle of scattering in the

[3] S. C. Snowdon, L. Eisenbud, and J. F. Marshall, J. Appl. Phys. **29**, 950 (1958).

center-of-mass system. Ordinates for determining these coefficients were read directly from smooth curves drawn through the data. The zirconium distribution displayed in Fig. 1 is a repetition of a previously published measurement.[4] It serves as a check of these earlier measurements against the improved geometry and data analysis subsequently adopted. The only significant change is an increase in magnitude of the first maximum to a value of 0.20 barn/sr.

B. Total and Integrated Cross Sections

Experimental total cross sections and integrated cross sections for the five new measurements described above are presented in Table II. Additional total cross-section measurements are included in Table III which summarizes all the total cross sections measured by us at 3.7 Mev. They are displayed as a function of atomic weight in Fig. 3, together with a similar plot for our nonelastic cross-section measurements at this energy. It is to be noted that measurements of $(n,n'\gamma)$ cross sections for Ca have been made,[5] indicating a minimum nonelastic cross section $\sigma_{\text{nonel}}=0.206\pm0.064$b, a value consistent with present measurements.

V. DISCUSSION

In predicting the position and magnitude of maxima in angular distributions of elastic scattering, it has proved helpful to consider a spin-orbit term in the nuclear potential. Preliminary calculations based on a potential which includes such a term have been made by Bjorklund[6] for comparison with our cross-section measurements of 3.7-Mev neutrons on nine medium weight nuclei. The potential has the form

$$V=V_{\text{cr}}\rho(r)+iV_{\text{ci}}q(r)+V_{\text{sr}}(\hbar/\mu c)^2\frac{d\rho(r)}{rdr}\boldsymbol{\sigma}\cdot\mathbf{L},$$

with $V_{\text{cr}}=47$ Mev, $V_{\text{ci}}=7$ Mev, $V_{\text{sr}}=8.7$ Mev, $a=0.65$f,

TABLE II. Experimentally determined total and integrated cross sections in barns. $E_n=3.66$ Mev.

Element	σ_{tot}	$\sigma_{\text{tot el}}$	σ_{nonel}
S	2.58±0.13[a]	1.80±0.08[a]	0.78±0.12[a]
K	3.48±0.24	3.08±0.24	0.40±0.30
Ca	3.58±0.18	3.09±0.21	0.49±0.25
Fe	3.41±0.14[a]	1.90±0.10[a]	1.51±0.17[a]
Ni	3.33±0.15[a]	1.82±0.10[a]	1.51±0.18[a]
Co	3.59±0.15[a]	1.97±0.10[a]	1.62±0.18[a]
Cu	3.38±0.15[a]	1.81±0.10[a]	1.57±0.18[a]
Zn	3.59±0.17[a]	1.75±0.10[a]	1.84±0.20[a]
Ge	3.67±0.18	1.70±0.13	1.97±0.22
Se	4.21±0.21	1.86±0.12	2.35±0.24
Sr	4.42±0.21	2.74±0.23	1.68±0.26
Zr	3.93±0.20	2.22±0.11	1.71±0.23

[a] Previously published measurement (see reference 2).

[4] H. S. Hans and S. C. Snowdon, Phys. Rev. **108**, 1028 (1957).
[5] R. B. Day, Phys. Rev. **102**, 767 (1956).
[6] F. E. Bjorklund (private communication).

and $b=1.0$f. The form factors are

$$\rho(r)=[1+\exp(r-R_0)/a]^{-1}$$

and

$$q(r)=\exp[-(r-R_0)^2/b^2],$$

where $R_0=1.25A^{\frac{1}{3}}$f. Preliminary calculations of the differential cross sections were made for germanium, selenium, and zirconium, and are included in Figs. 1 and 2 as dashed curves. An isotropically distributed component of 0.03 barn/sr has been arbitrarily added in each case in order to account in a rough way for compound elastic scattering.

The experimental variations of total and nonelastic cross sections as a function of atomic weight for a

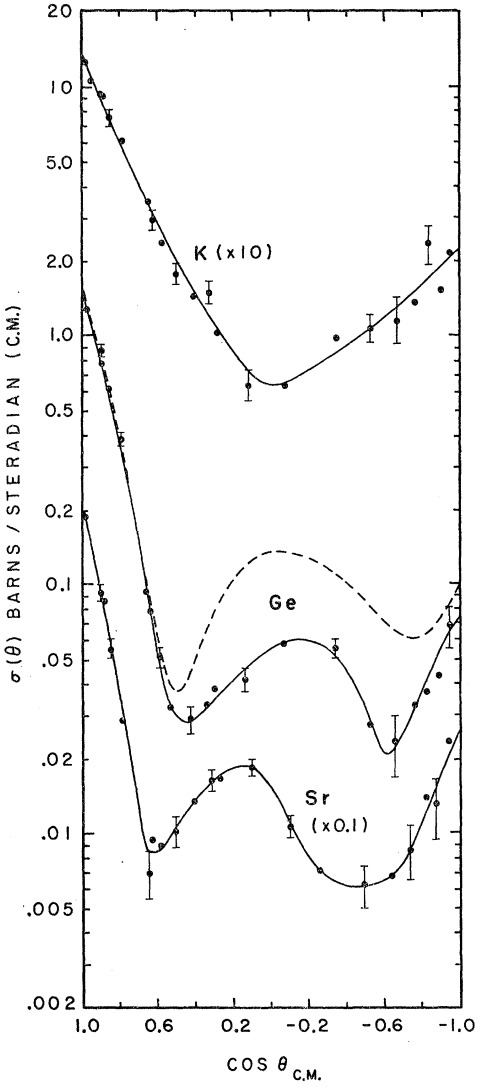

FIG. 2. Differential cross section for elastic scattering of 3.7-Mev neutrons from K, Ge, and Sr. Solid curves drawn through the data are used for determining the Legendre coefficients in Table I. The dashed curve is a preliminary fit for Ge by Bjorklund assuming $\sigma_{\text{ce}}(\theta)=0.03$ barn/steradian. Error bars are shown only on typical points to avoid cluttering of figure.

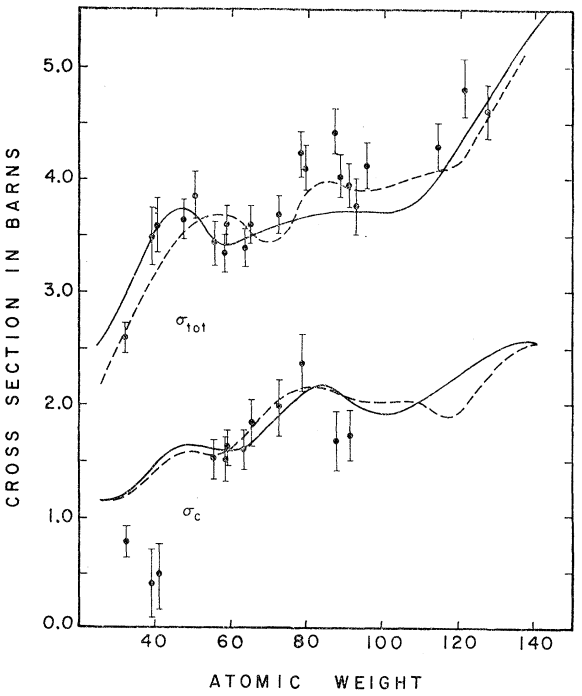

FIG. 3. Total and nonelastic cross sections for 3.7-Mev neutrons, compared with theoretical curves σ_{tot} and σ_c, the cross sections for total and compound nucleus formation, respectively. The solid curves are based on calculations by Emmerich,[8] while dashed curves are from calculations by Beyster *et al.*[7]

fixed neutron energy of 3.7 Mev are compared directly in Fig. 3 with two representative optical model predictions, using the cross section for compound nucleus formation as a comparison curve for the experimental nonelastic cross-section data. Spin-orbit terms were omitted for simplicity, since their contribution to these predictions is expected to be small. The dashed curves are obtained from calculations by Beyster et al.[7] who made detailed fits to a large body of data using the Woods-Saxon potential:

$$V=V_0(1+i\zeta)[1+\exp(r-R)/\tau]^{-1}.$$

Parameters were chosen for each element to obtain the best fits for that element at energies ranging from 0 to 14 Mev. The procedure involved adjustment of V_0 and ζ to fit data in a manner consistent with theoretical expectation. Their attention was directed first to high energies (greater than 4 Mev) before extending comparisons to lower energies where ambiguities arise from compound elastic contributions. The well depth ranged from 39 to 44 Mev, whereas ζ varied from 0.06 to 0.20. In the expression for nuclear radius, $R=r_0A^{\frac{1}{3}}$, r_0 varied from 1.450 f to 1.315 f, while the diffuseness parameter, a, varied from 0.35 f^{-1} to 0.50 f^{-1}.

The solid curves in Fig. 3 are predictions obtained from a calculation by Emmerich[8]; the real part of the potential is quite similar to that of Beyster *et al.*, but the imaginary part is concentrated near the surface. The four parameters which delineate the well shape and dimensions were chosen in this case to fit data for incident neutron energies from 1 to 14 Mev. The parameters were fixed for all values of A, and were varied with neutron energy. The mean radius was defined in this case by $\bar{R}=1.25A^{\frac{1}{3}}+0.5$ f. The well depth for the real part was held constant, at about 42 Mev, out to a critical radius defined by $R_c=\bar{R}-1.359\tau$. Beyond R_c, the well shape was described by a form factor (e^x-x), where $x=(r-R_c)/0.84$. The imaginary part was zero inside R_c, while outside it was proportional to the derivative of the real part with respect to x, the constant of proportionality being fixed at about $\lambda=0.39$.

Apart from the generally reasonable agreement with theory, there are some features which should be pointed out. Comparison of the two upper curves with experimental data in Fig. 3 indicates that, in the "plateau" region from $A=50$ to $A=110$, there is a discernible rise in the measured total cross section near $A=85$ which is only faintly indicated by the two calculations. In comparing our nonelastic cross-section data with the two lower curves representing predictions for the compound nucleus formation, a component of compound elastic scattering must be added to each data point.

In preliminary fits of the angular distribution data with Bjorklund's predictions, a rough value for the compound elastic scattering cross section $\sigma_{ce}=4\pi\times0.030=0.38$ b was assumed, indicating a reasonable fit to the experimental data for germanium, selenium, and zirconium. Our previous elastic scattering measurements[2] indicated that $\sigma_{ce}=4\pi\times0.023=0.29$ b was reasonable for comparison with predictions from a

TABLE III. Total cross-section measurements in barns. $E_n=3.66$ Mev.

A	Element	σ_{tot}	A	Element	σ_{tot}
32.07	S	2.58±0.13[a]	72.60	Ge	3.67±0.18
39.10	K	3.48±0.24	78.96	Se	4.21±0.21
40.08	Ca	3.58±0.18	79.92	Br	4.08±0.20
47.90	Ti	3.63±0.18	87.63	Sr	4.42±0.21
50.95	V	3.84±0.19	88.92	Y	4.01±0.20
55.85	Fe	3.41±0.14[a]	91.22	Zr	3.93±0.20
58.69	Ni	3.33±0.15[a]	92.91	Nb	3.75±0.25
58.94	Co	3.59±0.15[a]	95.95	Mo	4.11±0.21
63.57	Cu	3.38±0.15[a]	114.76	In	4.28±0.21
65.38	Zn	3.59±0.17[a]	121.76	Sb	4.78±0.24
			127.61	Te	4.58±0.23

[a] Previously published measurement (see reference 2).

[7] J. R. Beyster, R. G. Schrandt, M. Walt, and E. W. Salmi, Office of Technical Services Report LA-2099, 1957 (unpublished).

[8] W. S. Emmerich, Westinghouse Research Report 6-94511-6-R20, 1958 (unpublished).

potential containing no spin-orbit coupling term. If we then assign a somewhat arbitrary value of $\sigma_{ce}=0.35$ b for the range in atomic weights between $A=50$ and $A=100$, the predictions shown in Fig. 3 for compound nucleus formation are generally low by less than 0.5 b. Assuming that the predictions are also correct to this extent in the region extending down to $A=30$, we obtain a value of $\sigma_{ce}\approx 1.0$ b for sulfur, and $\sigma_{ce}\approx 1.5$ b for potassium and calcium.

ACKNOWLEDGMENT

We are grateful to Dr. F. Bjorklund for carrying out optical model calculations for germanium, selenium, and zirconium.

PHYSICAL REVIEW VOLUME 125, NUMBER 1 JANUARY 1, 1962

Resonant Scattering of Gamma Rays from Nuclear Levels with a Linear Accelerator

F. D. SEWARD
Lawrence Radiation Laboratory, University of California, Livermore, California
(Received August 11, 1961)

Several elements have been irradiated with a high-intensity bremsstrahlung beam and a search has been made for γ rays scattered from nuclear levels. A 6-in.×5-in.-diameter NaI(Tl) crystal was used as the detector. Resonant scattering was seen from Li^6, B^{11}, C^{12}, O^{16}, Mg, and Si. Pulse-height spectra for γ rays scattered from each of these are shown. Application of these spectra to previous experiments in which level widths and branching ratios were calculated is discussed. Levels in B^{11}, C^{12}, and O^{16} were observed which have not been seen with this technique previously.

INTRODUCTION

THE resonant scattering of gamma rays from nuclear levels has been observed by several techniques.[1] One method, which is the one used in the present study, is to place a sample of the scattering material in a high-energy bremsstrahlung beam. The bremsstrahlung spectrum is smooth and contains x rays of all energies up to the primary electron energy. If the scattering sample is viewed from the side, resonant-scattered gamma rays stand out from the background because they have a well-defined energy and because the cross section for the resonant process is quite large compared to that of nonresonant nuclear scattering and background effects.

In previous resonance fluorescence work of this type, mostly betatron work, a scattered photon spectrum has first been measured, and from this spectrum the presence of resonant-scattered γ rays and γ-ray branching ratios have been inferred. Scattered intensity measurements have then been made with good geometry, with and without an absorber in the incident beam, and the level widths calculated from this data.

In the experiment to be described an attempt was made to obtain scattered photon spectra with the best possible resolution. The linear accelerator provided a much more intense bremsstrahlung flux than betatrons of comparable energy. Scattered intensity and good geometry were sacrificed for resolution. Because of this and because of a slight energy fluctuation of the accelerator beam, no absorption measurements were undertaken. Since no absorption measurements were made and since the shape of the incident x-ray spectrum was not accurately known, level widths could not be calculated. However, the spectra obtained are better than those of previous work and some of the conclusions about branching ratios and level widths in Mg and Si are affected by the interpretation of these spectra.

This work then was intended to supplement previous measurements with better spectral data rather than to repeat the absorption measurements and level width calculations. It was also a survey to indicate other levels susceptible to this method of analysis. The following elements and compounds were used as scattering samples: Li^6H, Li^7, Be, B, B^{10}, C, H_2O, KF, NaCl, Mg, Al, Si, P, S, Ca, Ti, V, Cr, Mn, Fe, Co, Ni, Cu, and Zn. For each sample the scattered gamma spectrum was studied to determine energies and intensities of any resonant-scattered γ rays. Prominent scattered γ rays were seen from Li^6, B, C, O, Mg, and Si. Resonant scattering from other samples was too small to be distinguished from the background.

EXPERIMENTAL TECHNIQUE

The Livermore linear accelerator[2] is a pulsed machine and for this experiment was operated with a pulse length of 1 to 2 μsec and a repetition rate of 100 pulses per second. Average beam currents of 10 to 20 μamp were used. Electron energies ranged from 13 to 20 Mev, and the energy spread of the beam in this range was $\sim$2 Mev.

Bremsstrahlung x rays were produced by the electron beam striking a 0.10-in. Ta target backed by 2 in. of Al.

[1] S. Devons, in *Nuclear Spectroscopy*, edited by F. Ajzenberg-Selove (Academic Press, Inc., New York, 1960), Part A, p. 533.

[2] N. Austin and S. Fultz, Rev. Sci. Instr. **30**, 284 (1959).